Laser Faraday rotation measurement of current density fluctuations and electromagnetic torque (invited)

W. X. Ding,[a] D. L. Brower, and B. H. Deng
Electrical Engineering Department, University of California-Los Angeles, Los Angeles, California 90095

D. Craig, S. C. Prager, and V. Svidzinski
Physics Department, University of Wisconsin-Madison, Madison, Wisconsin 53706

(Presented on 19 April 2004; published 1 October 2004)

Far-infrared laser polarimetry with time response up to ~1 μs and spatial resolution ~8 cm has been successfully implemented on the Madison Symmetric Torus reversed-field pinch. Internal magnetic field and current density fluctuations are nonperturbatively measured. This is accomplished by taking parallel polarimetry chords which measure the line-integrated magnetic field fluctuations via Faraday rotation. With suitable analysis we are able to obtain information on spatial profiles of magnetic field fluctuations and current density fluctuations. Coherent interaction between these fluctuations is also measured and observed to generate an electromagnetic fluctuation-induced torque $\langle \delta \mathbf{J} \times \delta \mathbf{B} \rangle$. © *2004 American Institute of Physics*.
[DOI: 10.1063/1.1785275]

I. INTRODUCTION

In high-temperature plasmas, the magnetic field and current density fluctuate spontaneously in space and time. This can result in magnetic field lines wandering stochastically in space, causing stochastic particle trajectories which lead to the anomalous transport of particles, momentum, and energy. Energy transport and dynamo effects from magnetic field fluctuations are especially crucial to the reversed-field pinch (RFP) laboratory plasma configuration. It has long been considered that transport arises from stochasticity induced by overlapping magnetic islands, and that the current density profile is partly determined by the dynamo effect.

Understanding transport physics and magnetic reconnection requires measurement of magnetic field fluctuations and current density fluctuations in the high-temperature plasma interior. It is of particular importance to measure the current sheet width which controls the magnetic reconnection rate. Current density fluctuations can also induce torque along the mean magnetic field, which results in plasma momentum transport. While global magnetic fluctuation spectra can be inferred from magnetic coils mounted on the wall, it is difficult to measure current density fluctuations since they are localized to the hot plasma interior.

Recently, a new high-speed laser polarimeter system[1] has been developed on the Madison Symmetric Torus (MST) RFP. Fast time response (up to ~1 μs) and good phase resolution allow us to probe internal magnetic fluctuations without perturbing the plasma. Due to the line-integrated nature of the fluctuation measurements, it is important to develop proper inversion techniques so that the spatial profile of magnetic fluctuations and associated current density fluctuation can be obtained. However, the conventional Abel inversion approach widely used for reconstruction of the equilibrium profile is ***not*** directly applicable to the reconstruction of the fluctuation profile since fluctuation quantities are not generally a function of flux surface. In this article, we present analysis techniques that allow us to infer information on spatial profiles of magnetic field fluctuations and current density fluctuations. With this information, we can identify the coherent interaction between these fluctuations and determine the electromagnetic fluctuation-induced torque $\langle \delta \mathbf{J} \times \delta \mathbf{B} \rangle$.

The remainder of the article is organized as follows: in Sec. II the laser-based Faraday rotation measurement is briefly described; in Sec. III magnetic fluctuation measurements are presented; in Sec. IV current density fluctuation measurement and inversion is described; in Sec. V spatial profile for magnetic and current density fluctuations is shown and electromagnetic fluctuation-induced torque is evaluated, and Sec. VI is a discussion of results and summary.

II. LASER FARADAY ROTATION MEASUREMENT METHOD

It is well known that a linearly polarized laser beam will experience a change in its polarization direction upon propagation along a magnetic field in a plasma. This is referred to as the Faraday effect. Faraday rotation in plasmas arises from the fact that left-hand (L wave) and right-hand (R wave) circularly polarized waves have different velocities (or different refractivity). The Faraday rotation measurement technique has been previously described[1,2] and Fig. 1 provides an overview of the experimental setup. The multiwave laser with nominal wavelength $\lambda_0 \sim 432$ μm consists of an R-wave (E_R, ω_1) and L wave (E_L, ω_2) that collinearly propagate through the plasma with slightly different frequencies, $\Delta\omega = |\omega_1 - \omega_2| \ll \omega_{pe}$, $\omega_{ce} \ll \omega_1 \sim \omega_2 \sim \omega$. Here ω_{pe} and ω_{ce} are electron plasma frequency and gyrofrequency, and E is their amplitude. Schottky-diode mixers are used to detect radiation from these beams and generate an intermediate-

[a]Electronic mail: wding@wisc.edu

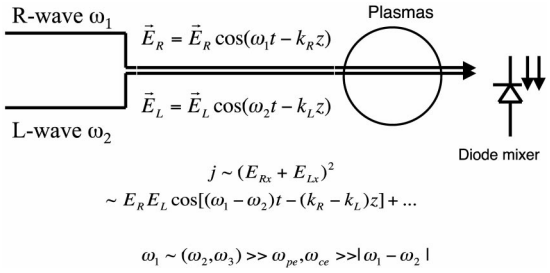

FIG. 1. The principle of laser Faraday rotation measurement.

frequency signal $\sim E_R E_L \cos[(\omega_1-\omega_2)t-(k_R-k_L)z]$ which is compared to a reference signal without plasma so that the phase $(k_R-k_L)z$ can be obtained. From the dispersion relation of the two waves, we know

$$k_L(\omega_1) - k_R(\omega_2) = \frac{\omega_1}{c}\left(N_L - \frac{\omega_2}{\omega_1}N_R\right) \approx \frac{\omega^2_{\mathrm{pe}}\omega_{\mathrm{ce}}}{c\omega^2} \sim n_e B_z. \tag{1}$$

Thus, the Faraday rotation angle Ψ is half of the phase difference between the R and L waves leading to

$$\begin{aligned}\Psi &= \frac{2\pi}{\lambda}\int \frac{(N_R - N_L)}{2} dz \\ &= 2.62 \times 10^{-13}\lambda^2 \int n_e B_\theta \cos\theta dz \\ &= c_F \int n_e \mathbf{B}\cdot d\mathbf{z},\end{aligned} \tag{2}$$

where B is magnetic field strength, n_e is the electron density, λ is the laser wavelength, θ is the angle between the magnetic field and the laser beam, and z is the plasma cross section vertical coordinate, all in MKS units. It is convenient to write Eq. (2) in the form of $\int n_e \mathbf{B}\cdot d\mathbf{l}$ in order to directly use Ampere's law to measure current as will be discussed later. The average phase of the R- and L-waves gives the electron density according to the conventional interferometer relation

$$\Phi = \frac{2\pi}{\lambda}\int \frac{N_R + N_L}{2} dz \approx 2.82 \times 10^{-15}\lambda \int n_e(z) dz. \tag{3}$$

The vertically viewing polarimeter–interferometer system consists of 11 chords divided between toroidal azimuths 250° (five chords located at $x=R-R_0=36$, 21, 6, −9, and −24 cm) and 255° (six chords located at $x=R-R_0=43$, 28, 13, −2, −17, and −32 cm). Although the polarimeter has been operated with time response up to 1 μs, full bandwidth is not required for the measurements presented here. Since the rms noise level varies with bandwidth, it is adjusted according to experimental demands in order to optimize the measurement. Typical polarimeter system rms noise levels are 1 mrad (≈0.1°) at 100 kHz bandwidth and 0.4 mrad (0.04°) at 20 kHz bandwidth. Data have been ensemble averaged over 380 independent sawtooth events for further noise reduction.

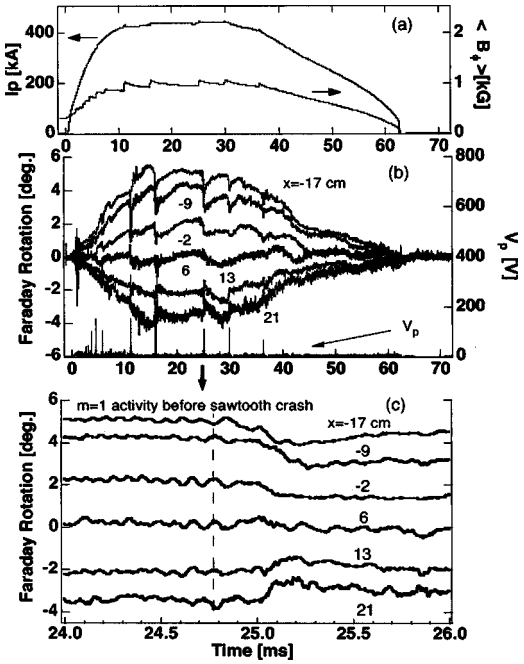

FIG. 2. (a) Discharge current and averaged toroidal flux; (b) time history of Faraday rotation angle; and (c) coherent oscillation of Faraday rotation angle corresponding to magnetic fluctuation.

III. MAGNETIC FLUCTUATION MEASUREMENTS

Experiments have been performed on the MST RFP, a device with with major radius $R=1.5$ m, minor radius $a=0.52$ m, discharge current $I_p=350-400$ kA, line-average electron density $n_e \sim 1\times 10^{19}$ m^{-3}, and electron temperature $T_e \sim 300$ eV. Typical MST fast-polarimetry data for a sawtoothing discharge are shown in Fig. 2. As expected, the Faraday rotation angle changes sign about the magnetic axis due to a change in the direction of the equilibrium poloidal magnetic field with respect to the polarimeter chords [see Fig. 2(b)]. Zero Faraday rotation angle indicates that the probing beam passes through the magnetic axis. Each chord shows distinct sawtooth cycles, corresponding to changes in the equilibrium (axisymmetric) magnetic field. Sawtooth crashes, characterized by changes in toroidal flux, are denoted by prompt increases in the average toroidal field $\langle B_\phi \rangle$ [see Fig. 2(a)].

To examine fluctuations in the Faraday rotation signals, we expand the time axis and isolate an individual sawtooth crash ($t=25$ ms) as shown in Fig. 2(c). The sawtooth crash or relaxation time scale is ≈100–200 μs. A clear coherent oscillation is observed on all chords prior to the sawtooth crash. The frequency (~12 kHz) of these fluctuations matches the dominant $m=1$ tearing mode in MST (as measured by external magnetic coils). The fluctuating component of the Faraday rotation signal can be written as[1,3]

$$\tilde{\Psi}(\tilde{n},\tilde{B}_z) = c_F\left(\int \tilde{n}B_{z0}dz + \int n_0\tilde{B}_z dz\right), \tag{4}$$

where the second order term, $c_F\int \tilde{B}_z\tilde{n}dz$, is negligible because both $\tilde{n}$ and $\tilde{B}_z$ are small. From this equation we see that the fluctuating part of the Faraday rotation signal is the sum of the fluctuating electron density weighted by equilibrium

magnetic field $\tilde{\Psi}(\tilde{n})$, and the fluctuating magnetic field weighted by equilibrium density $\tilde{\Psi}(\tilde{B}_z)$.

The first term of Eq. (4), $\int B_{0z}\tilde{n}dz$, resulting from electron density fluctuations, can be obtained by measurement of both the equilibrium magnetic field and electron density fluctuations. Equilibrium poloidal magnetic field near the magnetic axis in MST can be approximately represented as follows:[4,5]

$$B_\theta(r) \cong \mu_0 J(0)\frac{r}{2} \quad r \leqslant 0.3a, \tag{5}$$

where $J(0)$ is the equilibrium current density at the magnetic axis. Using polarimetry chords with $x \leqslant 0.3a$, we can estimate the density fluctuation contribution to the Faraday rotation signal as

$$\begin{aligned}\tilde{\Psi}(\tilde{n}) &= c_F \int \tilde{n}B_{z0}dz \\ &= c_F \int \tilde{n}B_\theta \cos\theta\, dz \leqslant c_F \int \left(\mu_0 J(0)\frac{r}{2}\right)\frac{x}{r}\tilde{n}\, dz \\ &= c_F \frac{\mu_0 J(0)}{2} x \int \tilde{n}\, dz. \end{aligned} \tag{6}$$

When the probe beam passes through the magnetic axis ($x=0$), Eq. (6) goes to zero. For $x \leqslant 0.3a$, $\int \tilde{n}\, dz \leqslant 0.5 \times 10^{17}\ \mathrm{m}^{-2}$ for dominant $m=1$ modes as measured by interferometry.[6] Consequently, Eq. (6) gives less than 0.01° for each of the chords shown in Fig. 2. This level is smaller than the system rms noise level. For the edge Faraday rotation chords, magnetic fluctuations are masked by large density fluctuations and special care is required to extract the magnetic fluctuation information.

In this article the six central chords, where density fluctuations are negligible, will be used to obtain magnetic fluctuation information. Equation (4) can then be rewritten as

$$\tilde{\Psi}(\tilde{n},\tilde{B}) \approx \tilde{\Psi}(\tilde{B}) = c_F \int n_0 \tilde{\mathbf{B}} \cdot d\mathbf{z} \approx c_F \bar{n}_0 \int \tilde{B}_z dz. \tag{7}$$

Taking $\tilde{\Psi} = \int n_0 \tilde{B}_z dz \approx \bar{n}_0 \int \tilde{B}_z dz$ is a good approximation for MST plasmas where the electron density profile is flat in the core and the fluctuating magnetic field falls off rapidly towards the wall. Therefore, measured Faraday rotation fluctuations provide a direct line-integrated measurement of magnetic fluctuations, where $\tilde{B}_z = \delta b_r \sin\theta + \delta b_\theta \cos\theta$ is the line-integrated magnetic fluctuation amplitude. Using the measured line-averaged density ($\bar{n}_0$), chord length (Δz), and Faraday rotation fluctuation level for the chord at $x=0$, we find the time-averaged rms amplitude of the radial magnetic field fluctuations, $\tilde{\bar{B}}_r \sim 33$ G or $\tilde{\bar{B}}_r / B_0 \sim 0.6\%$.

IV. CURRENT DENSITY FLUCTUATION MEASUREMENT

The line-integrated fluctuation measurement has to be inverted in order to obtain the magnetic fluctuation spatial profile. In general, this line-integrated measurement contains changing contributions of radial (δb_r) and poloidal (δb_θ) magnetic fluctuations along the probe beam path (except for the central chord which measures δb_r). There is no established technique for inverting the line-integrated measurement in order to obtain the magnetic fluctuation spatial profile. In the following, we present a method to obtain the local magnetic and current density fluctuation spatial profiles.

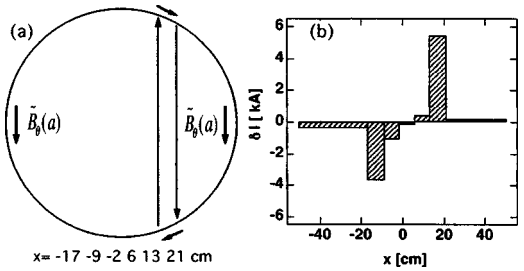

FIG. 3. (a) The D-shaped loop formed by a pair of polarimetry chords used to infer current flowing through it and (b) measured current fluctuation distribution.

Low-frequency magnetic fluctuations (5–30 kHz) in MST are known to be tearing modes and are generally observed in all toroidal confinement plasmas. The global magnetic field fluctuations are generated by current fluctuations in the vicinity of the resonant surface where there is finite resistivity. Our approach involves determining the current fluctuation instead of inverting δb_r and δb_θ. The fluctuating toroidal current ($\tilde{I}_\varphi$) can be estimated using Ampere's law

$$\oint_L \tilde{B} \cdot d\mathbf{l} \approx \left[\int \tilde{B}_z dz\right]_{x1} - \left[\int \tilde{B}_z dz\right]_{x2} \approx \mu_0 \tilde{I}_\phi, \tag{8}$$

where L represents the closed loop formed between any two chords as shown in Fig. 3(a). Contributions from the portion of the loop along the plasma edge but between the chords are negligible due to both the short distance and small fluctuation amplitude. These two integrals can be evaluated by using the Faraday rotation fluctuation measurements according to Eq. (5).[1] Thus one can directly rewrite Eq. (6) giving

$$\delta I_\phi \approx \int_{x_1} \delta\mathbf{B} \cdot d\mathbf{l}' - \int_{x_2} \delta\mathbf{B} \cdot d\mathbf{l} = \Delta\tilde{\Psi}/c_F \bar{n}_e \mu_0. \tag{9}$$

From this relation we see that the current fluctuations in the region between two chords is proportional to the difference in Faraday rotation fluctuations. Equation (9) establishes a direct relationship between the fluctuating current and the measured Faraday rotation fluctuations. The nonperturbing loop formed by a pair of polarimety chords is similar to a Rogowski coil used to measure discharge current. By taking the loop between the adjacent pairs of chords [using the data in Fig. 2(c)], the spatial distribution of the fluctuating current can be obtained as shown in Fig. 3(b).[1] The measured current fluctuations can be decomposed into modes of specific helicity (m,n) by correlating the Faraday signals with a magnetic coil array which isolates the various Fourier components of the magnetic fluctuations.

Local current density fluctuation $\delta j_\phi(r)$ can be obtained by inverting the measured current fluctuation $\delta I_\phi(x)$ distribution. In general, the toroidal fluctuating current density has a helical form $\delta j_\phi = \delta j_\phi(r)\cos(m\theta + n\phi)$. Toroidal effects are

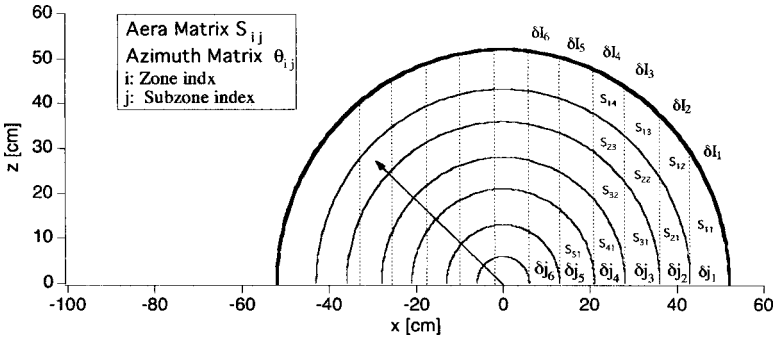

FIG. 4. Area matrix formed by flux surface and polarimetry chords. Here only half the cross section of MST is shown.

considered to be modest in the RFP since the toroidal magnetic field is comparable to the poloidal magnetic field. For the dominant, core-resonant, $(m,n)=(1,6)$ mode in MST, we wish to determine the $\delta j_\phi(r)$ profile where $\delta j_\phi(r)$ is the current density fluctuation on the mid-plane. The current density fluctuation can be directly inverted by employing a heuristic method as described in the following. Figure 4 shows a poloidal cross section of MST where the concentric circles represent flux surfaces and the $m=1$ mode amplitude is symmetric about the mid-plane. Vertical dashed lines correspond to Faraday rotation measurement chords. An area matrix, S_{ij}, is formed by the intersecting lines and curves. Since the fluctuating current is not a flux function, we have to invert the outboard and inboard sides independently to obtain the local current density. By definition, $\delta j_1=2(\delta I_1/S_{11})$. Note that $\delta I_1=(1/\mu_0)(\int \tilde{B}_z dz-2b_\theta(a)L_1)$ and L_1 is the arc length forming area S_{11}. Current flowing in the area S_{12} will be $(\delta j_1 \cos\theta_{12})\times S_{12}$, where θ_{12} is the azimuth of area element S_{12}. Then $\delta j_2=2(\delta I_2-\delta j_1 \cos\theta_{12}S_{12})/S_{21}$, moving on toward the core region, one obtains the $\delta j(r)$ profile as follows:

$$\delta j_1 = 2\frac{\delta I_1}{S_1},$$

$$\delta j_2 = 2\frac{1}{S_2}(\delta I_2 - \delta j_1 \cos\theta_{12}\times S_{12}),$$

$$\delta j_3 = 2\frac{1}{S_3}(\delta I_3 - \delta j_1 \cos\theta_{13}\times S_{13} - \delta j_2 \cos\theta_{23}\times S_{23}),$$

$$\cdots$$

$$\delta j_k = 2\sum_{k>l}^{l=1,k-1} M_{kl}\delta I_l. \tag{10}$$

Mathematically, we end up with a matrix M determined by area elements and azimuth of area. Similarly, one can start from the inboard side to invert $\delta j_\phi(r)$. This "onion-peel" method is similar to techniques for inversion of asymmetric density.[7] As long as the current fluctuations are known, local current density fluctuations can be obtained by using Eqs. (10). Experimentally, we observe that fluctuating current $\delta I_5(\gg \delta I_4, \delta I_3, \delta I_2, \delta I_1)$ dominates near the (1,6) resonant surface. This character greatly simplifies the inversion procedure. The inverted profile is shown in Fig. 5 and is quite similar to the current fluctuation profile of Fig. 3(b). The fluctuating current density peaks sharply at the resonant surface with amplitude $\delta j_\phi/J_0 \sim 5\%-6\%$ and spatial extent ~ 8 cm. Time evolution of current density fluctuation $\delta j_5 \approx \delta I_5/S_{51}$ near the (1,6) resonant surface can also be measured and is shown in Fig. 6. The current density fluctuation experiences a rapid growth immediately before and during the sawtooth crash. Current density fluctuations are well correlated to the mean current density dynamic.

V. MAGNETIC AND CURRENT DENSITY FLUCTUATION SPATIAL PROFILE

In principle, the magnetic fluctuation amplitude and spatial profile can be obtained by integrating the current density fluctuation. However, as discussed in Sec. IV, two conditions are required to obtain the MST current density fluctuation spatial profile: (1) density fluctuations must be small for the central chords and (2) the equilibrium density profile must be nearly flat. While these conditions are valid for the case discussed here, this may not be the case for all MST discharges (e.g., pellet injection) or in general for application of Faraday rotation on other toroidal confinement devices (e.g., tokamaks). Therefore, in order to determine more precisely the magnetic and current density fluctuation profiles for a

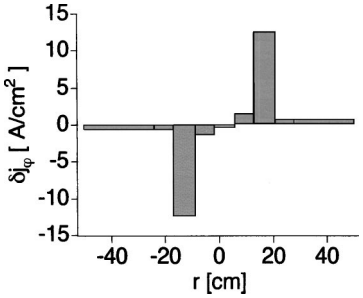

FIG. 5. Spatial profile of current density fluctuation from direct inversion.

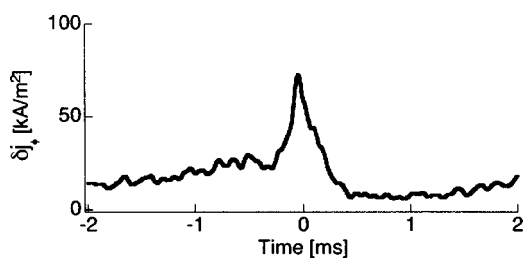

FIG. 6. Dynamics of current density fluctuation. Current density fluctuation suddenly increases approaching a sawtooth crash ($t=0$).

broader application, we have developed a simple fitting routine to invert both the magnetic field and current density fluctuation profiles.

According to standard resistive tearing mode theory, the current perturbation occurs in the vicinity of resonant surface. We assume that the resonant toroidal current density fluctuation profile has the form

$$\delta j_\phi(r) = j_a \exp\left(-\left(\frac{r-r_s}{w}\right)^2\right), \tag{11}$$

where j_a (amplitude), r_s (surface location), and w (width) serve as free parameters and $\delta j_\perp (\ll \delta j_\parallel) = 0$[8]. $\delta j_\theta(r)$ is not specified but it satisfies $\nabla \cdot \delta J = 0$. In general, one can specify the $\delta j_\theta(r)$ profile as well in order to compute the magnetic field fluctuations without assuming $\delta j_\perp (\ll \delta j_\parallel) = 0$. However, this will result in more free parameters to be determined by the fitting procedure and is presently not feasible using only the six central chords as constraints.

Once the fluctuating current density distribution is identified, the magnetic fluctuation spatial profile can be obtained by using $\nabla \times \delta B = \mu_0 \delta J$, $\nabla \cdot \delta B = 0$, and $\nabla \cdot \delta J = 0$. In cylindrical geometry with boundary condition $\delta b_r(a) = 0$ at conducting wall we have

$$\begin{aligned}
&\frac{1}{r}\frac{\partial}{\partial r} r \delta b_\theta - \frac{1}{r}\frac{\partial}{\partial \theta}\delta b_r = \mu_0 \delta j_\phi, \\
&\frac{1}{R}\frac{\partial}{\partial \phi}\delta b_r - \frac{\partial}{\partial r}\delta b_\phi = \mu_0 \delta j_\theta = -\mu_0 \frac{n}{m}\frac{r}{R}\delta j_\phi, \\
&\frac{\partial}{\partial r}\delta b_r + \frac{\partial}{r \partial \theta}\delta b_\theta + \frac{1}{R}\frac{\partial}{\partial \phi}\delta b_\phi = 0.
\end{aligned} \tag{12}$$

Magnetic field fluctuation profiles are obtained by numerically solving the above set of equations for a specified mode (m,n). A modeled Faraday rotation fluctuation for each chord is constructed as a function of the three free parameters as follows:

$$\tilde{\psi}^M(j_a, r_s, w) = c_F \int n_0(r)(\delta b_r \sin\theta + \delta b_\theta \cos\theta) dz. \tag{13}$$

Note that we use the measured equilibrium electron density profile rather than the line-averaged density. How well the modeled Faraday rotation fluctuations fit the experimental data is determined by computing χ^2 where

$$\chi^2 = \sum_{i=1}^{6} \frac{(\tilde{\Psi}_i(\tilde{B}) - \tilde{\psi}_i^M(j_a, r_s, w))^2}{\sigma_i^2} + \frac{(\delta b^M{}_\theta(a) - b_\theta(a))^2}{\sigma^2}, \tag{14}$$

and $\tilde{\Psi}_i(\tilde{B}) = (\tilde{\Psi}_i(\tilde{n}, \tilde{B}) - \tilde{\Psi}_i(\tilde{n}))$ is the measured Faraday rotation perturbation due to magnetic fluctuations, σ_i, σ are measurement errors, $b_\theta(a)$ is measured by magnetic coils mounted inside the vessel, and $b_\theta^M(a)$ is a modeled value. χ^2 is minimized by performing a scan of the free parameters (Amoeba routine in IDL program). As soon as the minimization is accomplished, the free parameters are determined. That is to say, the current density fluctuation and magnetic field fluctuation are determined. Initial selection of the free parameters is straightforward since we know the current density fluctuation peaks near the resonant surface from direct inversion of the current fluctuation as discussed in Sec. IV.

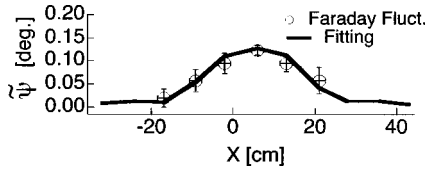

FIG. 7. Faraday rotation fluctuation amplitude for different chords. Circles represent measured Faraday rotation fluctuation. Solid line is fitting result.

The measured Faraday rotation fluctuation profile and best fit result are shown in Fig. 7, for the (1,6) mode. Only data from the six central chords are used for the fit because Faraday rotation fluctuations from the other chords are dominated by density fluctuations. Error bars for the experimental data are primarily ascribed to: (1) system calibration, (2) probing beam misalignment, and (3) rms noise of the detection system. For this best fit, the resulting magnetic field fluctuation and current density fluctuation spatial profiles for the dominant, core resonant, (1,6) mode are shown in Fig. 8. Although the current radial structure is localized, the $m=1$ character distributes current poloidally over a large region making the mode global. For a global mode, the use of multiple polarimeter chords enables us to spatially resolve the perturbed current profile.

Radial magnetic field fluctuations are observed to extend continuously through the rational surface indicating their resistive nature. Poloidal magnetic fluctuations change sign across the resonant surface. A maximum in the current density fluctuation $(\delta j_\phi / J_0 \sim 4.5\%)$ occurs at $r_s = 17$ cm where the (1,6) mode resonant surface is located based on equilibrium magnetic field measurements. The current density fluctuation obtained by this fitting procedure is in good agreement with the direct inversion result discussed in Sec. IV. The width of the current sheet is another important parameter that determines the mechanism of magnetic reconnection. Nonideal effects will expand the current sheet width to accelerate the magnetic reconnection rate. The fluctuating current channel radial width here is $\sim 8 \pm 3$ cm, which is approximately the ion skin depth (c/ω_{pi}) on MST.

To investigate what effect experimental errors have on determination of the current width, we study two adjacent loops with different fluctuating current $(\delta I_6, \delta I_5)$ which are measured as shown in Fig. 4. By varying the width used in

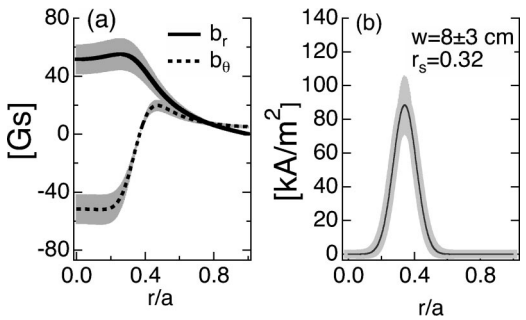

FIG. 8. (a) Radial and poloidal magnetic fluctuation spatial profile for dominant (1,6) mode and (b) corresponding current density fluctuation spatial profile.

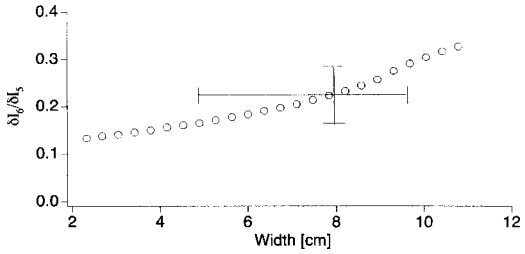

FIG. 9. The ratio of adjacent current fluctuations vs the width of current sheet. Uncertainty of current width is about ±3 cm when 25% error for current measurement is considered.

modeling and keeping r_s unchanged, we have a ratio of $\delta I_6/\delta I_5$ versus width as shown in Fig. 9. The ratio increases with width, being more sensitive to the larger width. A 25% experimental error in the current fluctuation ratio for width ~8 cm gives a width uncertainty of roughly (+2 cm, −3 cm).

Finally, with this measurement of δj_ϕ and δb_r, the electromagnetic torque,[8] $\langle \delta \mathbf{J} \times \delta \mathbf{B} \rangle$, can now be determined as shown in Fig. 10. A large increase in the fluctuation-induced torque is observed during a sawtooth crash and acts in the opposite direction of plasma motion. Future work on MST will focus on investigating how this torque affects the plasma electrons[9] (by driving a mean electric field via the Hall dynamo) and ions (via momentum transport).

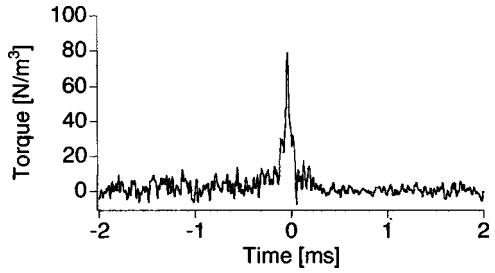

FIG. 10. Dynamics of plasma torque during a magnetic relaxation event. Time equal zero denotes the sawtooth crash.

VI. DISCUSSION

Faraday rotation fluctuations provide a direct probe of the fluctuating current due to the $\int n_e \mathbf{B} \cdot d\mathbf{l}$ nature of the measurement. With this understanding, the fluctuating current density spatial profile can be obtained. The magnetic fluctuation spatial profile can be determined by directly integrating the current density fluctuation. However, for broad application of Faraday rotation techniques to other confinement devices, we have developed a fitting procedure to invert the magnetic fluctuation spatial profile. Direct measurement of current density fluctuations in the high-temperature interior allows us to investigate current density fluctuation-induced plasma torque $\langle \delta J \times \delta B \rangle$, which plays an important role in plasma momentum transport. Measurement of the fluctuating current width also helps to reveal the underlying physics during magnetic reconnection.

ACKNOWLEDGMENTS

The authors gratefully acknowledge contributions from the MST group. This work is supported by the U.S. Department of Energy.

[1] D. L. Brower *et al.*, Rev. Sci. Instrum. **74**, 1534 (2003); W. X. Ding *et al.*, Phys. Rev. Lett. **90**, 035002 (2003).
[2] G. Dodel and W. Kunz, Infrared Phys. **18**, 773 (1978);J. H. Rommers and J. Howard, Plasma Phys. Controlled Fusion **38**, 1805 (1996).
[3] H. Soltwisch and H. R. Koslowski, Plasma Phys. Controlled Fusion **39**, A341 (1997).
[4] S. D. Terry *et al.*, Phys. Plasmas **11**, 1079 (2004).
[5] H. Soltwisch, Plasma Phys. Controlled Fusion **34**, 1669 (1992).
[6] N. E. Lanier *et al.*, Phys. Plasmas **8**, 3402 (2001).
[7] H. K. Park, Plasma Phys. Controlled Fusion **31**, 2035 (1989).
[8] R. Fitzpatrick, Nucl. Fusion **33**, 1049 (1993).
[9] W. X. Ding *et al.*, Phys. Rev. Lett. **93**, 045002 (2004).